SCIENCE CHINA
Physics, Mechanics & Astronomy

• News & Views •

November 2016 Vol. 59 No. 11: 114631
doi: 10.1007/s11433-016-0352-5

# Bridging length and time scales in moving contact line problems

YaPu Zhao[1,2*]

[1] State Key Laboratory of Nonlinear Mechanics, Institute of Mechanics, Chinese Academy of Sciences, Beijing 100190, China;
[2] School of Engineering Science, University of Chinese Academy of Sciences, Beijing 100049, China

Received August 31, 2016; accepted September 13, 2016; published online September 23, 2016

**Citation:** Y. P. Zhao, Bridging length and time scales in moving contact line problems, Sci. China-Phys. Mech. Astron. **59**, 114631 (2016), doi: 10.1007/s11433-016-0352-5

Physical, mechanical, chemical, and biological processes for various problems span length and time scales of many orders of magnitude [1-6]. As a typical dynamic process, moving contact line (MCL) problem or droplet spreading consists of 7-8 length and time scales from the atomistic to the continuum [2], as shown in Figure 1. A grand challenge in MCL problems is to link these vastly different length and time scales.

All these length and time scales origin from the competition among governing forces [7], which indicates that they can be bridged by specific dimensionless numbers, as listed in Table 1. The dimensionless numbers provide clear physical interpretation of MCL problems under study and also produce valuable scale estimates. Thus, we can choose the proper governing equations.

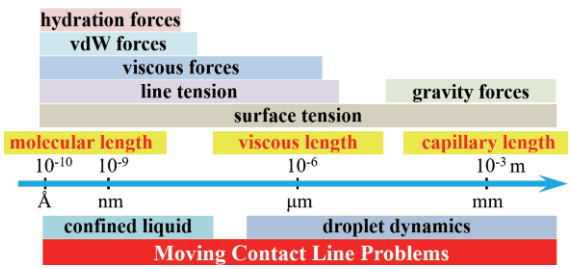


**Figure 1** (Color online) Schematic diagrams of various length scales in moving contact line problems. Ranges of several common forces at play in MCL problems are also illustrated.

As the first example, MCL consists of three regions as shown in Figure 2. In the macroscale region, when the droplet size is much less than the capillary length, the gravity forces is neglected compared with surface tension, which remarkably simplify the governing equations. In the mesoscale region, i.e. $L \approx 10^{-6}$ m or smaller, which is on the same order of magnitude of the viscous length, MCL is dissipated by the viscous resistance. It has been shown that in such region, the viscous dissipation results in significantly different droplet

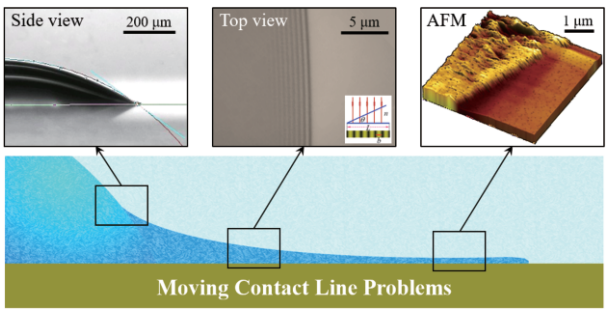


**Figure 2** (Color online) Different scales in MCL problems. Three insets show the experimental observation of the MCL using different facilities. Left: in the macroscale region, the contact angle of a water droplet with a base diameter of ~ $10^{-3}$ m can be measured using a droplet contour analyzer. Middle: in the mesoscale region, the edge shape of the droplet can be analysed using an optical microscope according to the interference in the liquid film. Right: in the microscale region, the most anterior part of the MCL was imaged by an atomic-force microscopy (AFM), when the liquid molecules or solvents have a distinguishable size compared with the roughness of the substrate.

*Corresponding author (email: yzhao@imech.ac.cn )

**Table 1** Characteristic length and time scales as well as interrelated Dimensionless numbers[a)]

| Length/time scales | Underlying forces | Dimensionless numbers |
|---|---|---|
| Capillary length | surface tension vs. gravity forces | Bond number ($Bo$): $Bo=\rho gL^2/\gamma_{lv}$, $L=\sqrt{\gamma_{lv}/\rho g}\approx 10^{-3}$ m |
| Viscous length | viscous forces vs. inertial forces and surface tension | Ohnesorge number (Oh): $Oh=\mu/\sqrt{\rho\gamma_{lv}L}$, $Oh\approx 0.1$, $L\approx 10^{-7}$ m |
| Molecular length | surface tension vs. van der Waals forces | Hamaker number ($Ha$): $Ha=A/(L^2\gamma_{lv})$, $L=\sqrt{A/\gamma_{lv}}\approx 10^{-10}$ m |
| Inertial characteristic length and time | viscous forces vs. inertial forces and surface tension | Ohnesorge number ($Oh$): $Oh\approx 0.1$, $L\approx 10^{-7}$ m, $\tau\approx 10^{-8}$ s |
| Relaxation time | viscous forces vs. inertial forces and surface tension | $L_{\text{water}}\approx 2.5\times 10^{-10}$ m, $\tau=L_{\text{water}}\mu/\gamma_{lv}\approx 3.46$ ps |
| Hydration length | surface tension vs. hydration forces | $L\sim 10^{-9}$ m |
| Droplet diameter | surface tension vs. inertial forces | Weber number ($We$): $We=\rho U^2L/\gamma_{lv}=\rho L^3/(\tau^2\gamma_{lv})$, $L=\gamma_{lv}/(\rho U^2)\approx 10^{-2}$ m, $\tau=\sqrt{\rho L^3/\mu}\approx 10^{-2}$ s |
| Channel size | inertial forces vs. viscous forces | Reynolds number ($Re$): $Re=\rho UL/\mu=\rho L^2/(\tau\mu)$, $L=\mu/(\rho U)\approx 10^{-5}$ m, $\tau=\rho L^2/\mu\approx 10^{-4}$ s |
| Elastocapillary length | surface tension vs. elasticity | $B/(L^2\gamma_{lv})$, $\gamma_{lv}\sin\theta/(GL)$, |
| Characteristic size | gravity forces vs. viscous forces | Galilei number ($Ga$): $Ga=\rho^2gL^3/\mu^2$, $L=\sqrt[3]{\mu^2/(\rho^2g)}\approx 10^{-5}$ m |
| Capillary time | surface tension vs. viscous forces | Capillary number ($Ca$): $Ca=\mu U/\gamma_{lv}=\mu L/(\tau\gamma_{lv})$, $\tau=\mu L/\gamma_{lv}\approx 10^{-5}$ s |
| Bjerrum length | electrostatic interaction vs. thermal energy | $L=e^2/(4\pi\varepsilon_0\varepsilon_r k_{\text{B}}T)\approx 7.1$ Å |
| Characteristic length | advective transport rate vs. diffusive transport rate | Péclet number ($Pe$): $Pe=LU/D=U^2\tau/D$, $L=D/U\approx 10^{-8}$ m, $\tau=D/U^2\approx 10^{-7}$ s |
| Thermal fluctuation length | thermal energy vs. surface tension | $L=\sqrt{k_{\text{B}}T/\gamma_{lv}}\approx 0.23$ nm |

a) $L$: characteristic length; $\tau$: characteristic time; $\rho$: density; $\gamma_{lv}$: surface tension; $U$: velocity; $\mu$: viscosity; $B$: bending modulus; $\theta$: contact angle; $G$: shear modulus; $g$: gravitational acceleration. $\varepsilon_0$: the vacuum permittivity; $\varepsilon_{\text{r}}$: relative permittivity; $D$: diffusion coefficient; $k_{\text{B}}$: the Boltzmann constant; $T$: absolute temperature. Length and times scales are estimated using $U$=0.1 m/s, $\rho=10^3$ kg/m$^3$, $\gamma_{lv}$=0.072 N/m, $\mu=10^{-3}$ Pa s, $D=2.299\times 10^{-9}$ m$^2$/s, which are typical for water at 25°C, 1 atm (1 atm=101325 Pa)

dynamics [8]. Under such circumstances, a term of viscous dissipation has to be added to the governing equations. So only the theoretical model can correctly reproduced the experimental results. In the microscale region, Hamaker number determines the molecular length of the precursor film [9]. Both the van der Waals interactions and nanoscale viscous dissipation play an important role [10]. It is an international puzzle to connect these scales, which is key to the "Huh-Scriven paradox".

The second example is about MCL in shale gas recovery,

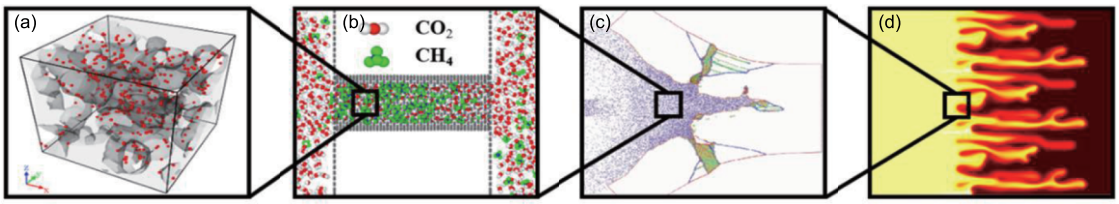


**Figure 3** (Color online) Different scales of MCL in shale gas recovery. (a) Kerogen decomposes into shale gas, which adsorbs on the wall of kerogen and shale, and forms micro-defects; (b) displacement of $CH_4$ by $CO_2$ in nano-pores; (c) hydraulic fracturing of shale; (d) fractal transport of shale gas in shale.

which spans several length and time scales. We used combined simulations of molecular dynamics (MD) and phase field (PF) to simulate these processes (Figure 3). Macroscale parameters are used as boundary and initial conditions in MD simulations, while microscale parameters are transferred to PF simulations to bridge scales. Over geologic time scales, the organic matter (kerogen) decomposes into shale gas under high crustal stress and temperature, which results in the formation of micro-defects. Then, the shale gas adsorbs on the wall of kerogen and shale (Figure 3(a)). To exploit the shale gas from shale, supercritical fluids [11,12], i.e. $CO_2$, $N_2$ and etc., are utilized to displace shale gas in channels (Figure 3(b)), which are formed by hydraulic fracturing of shale (Figure 3(c)) [13]. The dynamic properties of transport of supercritical fluids obtained from MD simulations are then transferred to the PF simulations at macroscale. Hence, the fractal and viscous fingering transport of shale gas in shale are captured in Figure 3(d).

Improvements of the experimental techniques have driven the research focus of MCL problems down to the nanoscale, which creates interesting new research opportunities. Some of the novel phenomena and emerging mechanisms expect new dimensionless numbers to understand the surface/interface effects with respect to MCL problems.

*This work was jointly supported by the CAS Key Research Program of Frontier Sciences (Grant No. QYZDJ-SSW-JSC019) and the Strategic Priority Research Program of the Chinese Academy of Sciences (Grant No. XDB22040401).*

1 Y. P. Zhao, *Physical Mechanics of Surfaces and Interfaces* (Science Press, Beijing, 2012).
2 Y. P. Zhao, Theor. Appl. Mech. Lett. **4**, 034002 (2014).
3 L. Y. Wang, F. C. Wang, F. Q. Yang, and H. A. Wu, Sci. China-Phys. Mech. Astron. **57**, 2152 (2014).
4 P. F. Hao, C. J. Lv, F. L. Niu, and Y. Yu, Sci. China-Phys. Mech. Astron. **57**, 1376 (2014).
5 P. F. Hao, C. J. Lv, Z. H. Yao, and F. L. Niu, Sci. China-Phys. Mech. Astron. **57**, 2127 (2014).
6 B. F. Zhang, K. Li, and J. Zhao, Sci. China-Phys. Mech. Astron. **57**, 1574 (2014).
7 G. W. Wang, Sci. China-Phys. Mech. Astron. **57**, 1569 (2014).
8 F. C. Wang, F. Yang, and Y. P. Zhao, Appl. Phys. Lett. **98**, 053112 (2011).
9 Q. Yuan, and Y. P. Zhao, Phys. Rev. Lett. **104**, 246101 (2010).
10 F. C. Wang, and Y. P. Zhao, Soft Matter **7**, 8628 (2011).
11 Q. Yuan, X. Zhu, K. Lin, and Y. P. Zhao, Phys. Chem. Chem. Phys. **17**, 31887 (2015).
12 K. Lin, Q. Yuan, Y. P. Zhao, and C. Cheng, Extreme Mech. Lett. in press, doi: 10.1016/j.eml.2016.05.014 (2016).
13 D. Li, F. C. Wang, Z. Y. Yang, and Y. P. Zhao, Sci. China-Phys. Mech. Astron. **57**, 2177 (2014).